Acta Crystallographica Section D
Biological Crystallography
ISSN 0907-4449

Physical aspects of protein crystal growth investigated with the Advanced Protein Crystallization Facility in reduced-gravity environments

Alessandro Vergara,[a] Bernard Lorber,[b] Adriana Zagari[c,d]* and Richard Giegé[b]

[a]Dipartimento di Chimica, Università di Napoli 'Federico II', Monte S. Angelo, 80126 Napoli, Italy, [b]Département des Mécanismes et Macromolécules de Synthèse Protéique et Cristallogenèse, UPR 9002, Institut de Biologie Moléculaire et Cellulaire du CNRS, 15 rue René Descartes, 67084 Strasbourg-Cedex, France, [c]Dipartimento di Chimica Biologica, Università di Napoli 'Federico II', Via Mezzocannone 6, 80134 Napoli, Italy, and [d]Istituto di Biostrutture e Bioimmagini, CNR, Via Mezzocannone 6, 80134 Napoli, Italy

Correspondence e-mail: zagari@chemistry.unina.it

Received 28 June 2002
Accepted 20 November 2002

The physicochemical aspects of protein crystallization in reduced-gravity environments (μ*g*) have been investigated with the Advanced Protein Crystallization Facility during six space missions. This review summarizes the results, dealing with the mechanisms of nucleation and crystal growth and with the quality of the crystals that were obtained under reduced gravity as well as under normal gravity on earth. Statistical analyses of the experimental data strongly support the fact that μ*g* has a positive effect on crystallization and on crystal quality. A comparison of experiments and theories of protein crystallization in reduced-gravity environments is presented. Recommendations for improving the performance of protein crystallization experiments in μ*g* and on earth are discussed.

1. Introduction

In structural biology, the last decade has seen significant advances in the performance of X-ray sources and detectors as well as in the capabilities of the hardware and software used by crystallographers to determine three-dimensional structures. Despite these improvements, production of well diffracting crystals of biological macromolecules remains a major impediment. Crystallization of these particles shares many common properties with that of small solute molecules (*e.g.* growth by two-dimensional nucleation or by screw-dislocation mechanisms), but their crystals exhibit several peculiarities: most of them have a high solvent content [*e.g.* 30–80%(*v*/*v*)], few intermolecular contacts and a high density of defects (Malkin *et al.*, 1996). Furthermore, macromolecular solutions are multi-component systems whose properties can be influenced by a variety of physical and chemical parameters (McPherson, 1993). As a result, study of their crystallization has become a natural science.

The purpose of any crystallization technique is to favour crystal nucleation by driving a solution from undersaturation to high supersaturation (this is the actual driving force). Once crystals grow, the concentration of soluble macromolecules and the supersaturation decrease. After some time, an equilibrium is reached, growth ceases and the concentration of soluble macromolecules becomes equal to the solubility. Fig. 1 displays examples of pathways followed by a given macromolecular solution during crystallization using the most widely used techniques. These are based on the batch (BAT), dialysis (DIA), free-interface diffusion (FID) or vapour diffusion (VD) principles (Chayen, 1998). Along these pathways, physical chemical processes such as nucleation, crystal growth and mass transport occur. In all cases, the gravity vector plays an important role, since on earth any inhomogeneity in the sample composition and hence in the density (at constant temperature) triggers convective flow which initiates mixing.

Alessandro Vergara is a Research Assistant of Physical Chemistry at the University of Naples "Federico II", where he graduated in Chemistry in 1996. He has been a post-doctoral fellow in Naples with Professor Zagari. Bernard Lorber is a biochemist and physico-chemist, Chargé de Recherches at CNRS, working with Richard Giegé at "Institut de Biologie Moléculaire et Cellulaire", Strasbourg, to understand the crystallogenesis of biomacromolecules. Adriana Zagari is a full Professor of Structural Chemistry at the University of Naples "Federico II". Her main interests are in protein crystallization and structural biology. Richard Giegé is a Directeur de Recherche at CNRS. Beside crystallogenesis, his main interests are in the structural and molecular biology of genetic code expression at the translational level. All authors conducted experiments in microgravity on several space missions, investigating the chemico-physical aspects of protein crystal growth.

Table 1
Space missions carrying APCF as a payload.

Mission	Flight(s)	Date	Proteins/ reactors	Active phase	Monitoring	Orbiter
SpaceHab-01	STS-57	June 1993	6/48	7 d 10 h	Video	Shuttle
IML-2	STS-65	July 1994	21/96	12 d 11 h	Video	Shuttle
USML-2	STS-73	October 1995	28/96	14 d 11 h	Video	Shuttle
LMS	STS-78	June 1996	12/96	15 d 10 h	Video/MZI	Shuttle
STS-95	STS-95	October 1998	14/90	8 d	Video/MZI	Shuttle
ISS-3	STS-105/ 108	August 2001	14/48	3 m 15 d	Video/MZI	ISS
STS-107	STS-107/ 110	January 2003	—	Scheduled	Video/MZI	Shuttle docked on ISS

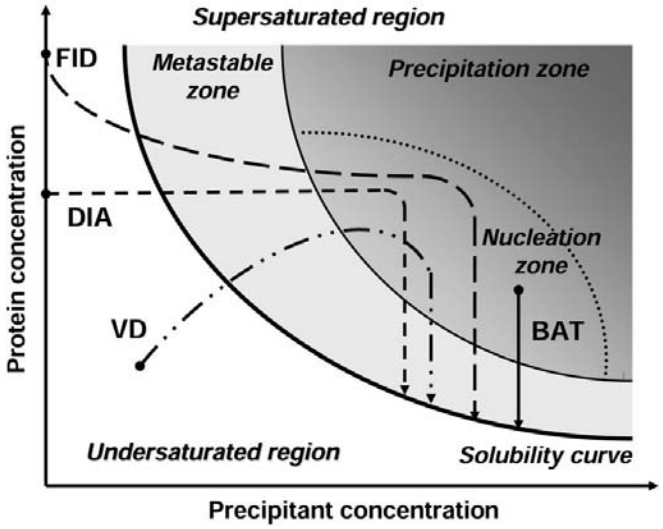

Figure 1
Equilibration pathways within the various APCF reactors. Theoretical two-dimensional phase diagram displaying how supersaturation is reached to trigger crystallization in VD, DIA, FID and BAT reactors (after Chayen, 1998).

At this point, a reduction in the level of gravity has a potential advantage, as buoyancy-driven convection and sedimentation are, in principle, suppressed at zero gravity. Aboard an orbiter, such as a space shuttle or a space station, reduced-gravity environments exist ($\mu g \simeq 10^{-3}$–$10^{-6}g$) in which diffusive transport is dominant. Since most protein molecules have diffusivities of $\sim 10^{-6}$–10^{-7} cm^2 s^{-1} (Albright *et al.*, 1999; Petsev *et al.*, 2000), they will move more slowly and hence may have a higher probability of being incorporated at a uniform rate in the correct orientation on a crystalline surface. In a quasi-containerless system, the simultaneous absence of convection and of sedimentation minimizes the probability of nucleation (resulting in a small number of larger crystals) and favours isotropic growth. From a practical point of view, the crystallization techniques used on earth can be applied to experimentation in reduced gravity with small sample volume and minimal intervention. These physical and operational considerations motivated the pioneering experiments to crystallize proteins in μg (Littke & John, 1984). Since then, numerous more-or-less sophisticated instruments have been designed and built. One of them, the Advanced Protein Crystallization Facility (APCF) (Snyder *et al.*, 1991; Bosch *et al.*, 1992*b*) can use four techniques, can handle a broad range of sample volumes and can monitor the crystallization process with a video camera and an interferometer (Snell, Helliwell, Boggon *et al.*, 1996). A lighter version, the Commercial Protein Crystallization Facility (CPCF), utilizes the same reactors without any means of observation (Stapelmann *et al.*, 2001). It was recently used on the International Space Station (ISS) (Borgstahl *et al.*, 2001; Pletser *et al.*, 2001*a*,*b*).

This review is intended to summarize the results in the field of the physics of crystal growth that were essentially obtained with the APCF on six space missions (Table 1). Other reviews of crystallization experiments carried out in μg have reported partial results obtained with the APCF (Giegé *et al.*, 1995; McPherson, 1996; Snell *et al.*, 1999; DeLucas, 2001; García-Ruiz, Drenth *et al.*, 2001; Giegé & McPherson, 2001; Kundrot *et al.*, 2001; Lorber, 2002). Details of results obtained in the field of structural determination will be presented elsewhere. Since experiments in μg are of no value if they are not accompanied by control experiments performed in parallel on earth, our attention was primarily focused on the cases where results were available for comparison. Also, experiments performed under conditions mimicking in part μg on earth by creating an environment in which convection and sedimentation are minimized will be treated. They include crystallization in gels (Ducruix & Giegé, 1999) and in mixtures of oil (Chayen *et al.*, 1990; Lorber & Giegé, 1996; Chayen, 2002). Techniques using magnetic fields (Lin *et al.*, 2000) or high gravity (Pjura *et al.*, 2000) will be mentioned. The contribution of the investigations conducted with the APCF to the knowledge of protein crystallization in μg and on earth will be discussed.

2. APCF

2.1. Design of the instrument

The APCF was built by Astrium GmbH (formerly Dornier GmbH) under a contract from the ESA (Snyder *et al.*, 1991; Bosch *et al.*, 1992*a*,*b*); it measures 500 × 400 × 240 mm, weighs 26 kg and consumes a maximum of 65 W. It operates fully automatically after switch-on and is controlled by a 16-bit microprocessor. One APCF unit accommodates up to 48 reactors that measure 54 × 45 × 18 mm each and are made of quartz glass and aluminium alloy. The protein volume per reactor ranges from 4 to 470 µl. Chambers of DIA and FID reactors have plane surfaces for distortion-free optical observation. The VD, DIA and FID reactors are shown in Fig. 2. Because of Marangoni convection (at the air–solution interface) and poor image quality (owing to the cylindrical geometry of the protein chamber), the VD technique was abandoned prior to the STS-95 mission. On the other hand, XL-FID reactors with a longer protein chamber were developed for the STS-95 mission to take advantage of counter-diffusion methods (Sauter *et al.*, 2001). Ortho-FID reactors were designed for observation along two orthogonal direc-

tions. The video system can monitor 2 × 6 reactors. The camera consists of a black-and-white charge-coupled device (CCD; 5000 × 582 pixels), with optics providing either a narrow or wide field of view covering 5.0 × 3.7 or 8.6 × 6.4 mm, respectively. A light-emitting diode illuminates the samples with polarized light. The video recorder (200 × 140 × 180 mm) has a capacity of 5 Gb and can store 15 000 video images with housekeeping data. For the LMS mission, a Mach–Zehnder interferometer (MZI) (Fig. 3) was added to observe the refractive-index profile around crystals in five of the 48 reactors (Snell, Helliwell, Boggon *et al.*, 1996). This final configuration of the APCF was used on all missions after the IML-2.

2.2. Experimentation in space and on earth

On the six missions, pre-flight experimentation was devoted to optimizing the crystallization conditions while meeting the requirements with respect to reactor geometry and active-phase duration. On each mission, all reactors were available in duplicate for control experiments on earth under otherwise identical conditions, in parallel with the experiments in space. The flight reactors were filled under the supervision of Astrium GmbH either at CNRS in Strasbourg, at EMBL in Hamburg or at NASA's Kennedy Space Center in Florida. They were shipped to the launch site in a thermostated box and photographed prior to their installation into the APCF. On five of the missions the instrument was located in a mid-deck locker of the shuttle and on the sixth mission it was transferred onboard the ISS (Table 1). All reactors were activated simultaneously under μ*g* by rotating their plug by 90° to bring into contact the content of the protein and buffer and/or precipitant chambers (Fig. 2). Video and MZI images were recorded in space. At the end of the microgravity session, rotating the plug in the opposite direction inactivated the reactors. The protein chambers were photographed after landing and before returning the reactors to investigators. Afterwards, the video and/or MZI images were distributed to investigators. X-ray diffraction data collection was performed by the individual investigators as soon as possible, at synchrotron beamlines for most samples.

3. How protein crystallogenesis is studied

Many physical methods have been applied to investigate protein crystal growth or to assess crystal quality. We mention those adopted to analyze μ*g*-grown crystals or to understand the μ*g* effect on protein crystallization.

3.1. Pre-crystallization

Static or dynamic light scattering (SLS or DLS) and small-angle light, neutron or X-ray scattering (SALS, SANS and SAXS, respectively) can provide information about molecular interactions in solution. SLS provides the second virial coefficient, related to the derivative of the protein chemical potential with respect to the protein concentration C_P. This coefficient is also related to the driving force of nucleation and crystal growth (George *et al.*, 1997 and references therein; Petsev *et al.*, 2000). SALS studies have provided evidence of giant fluctuations in free-diffusion processes in the presence of large concentration gradients (Valiati & Giglio, 1997) (as in FID or DIA experiments) that are usually damped by gravity and are expected to become important in μ*g* (Valiati & Giglio, 1998). SANS and SAXS provide the sizes and shape factors of particles and can yield the second virial coefficient (Tardieu *et al.*, 1999; Vidal *et al.*, 1998; Vivarès & Bonneté, 2002).

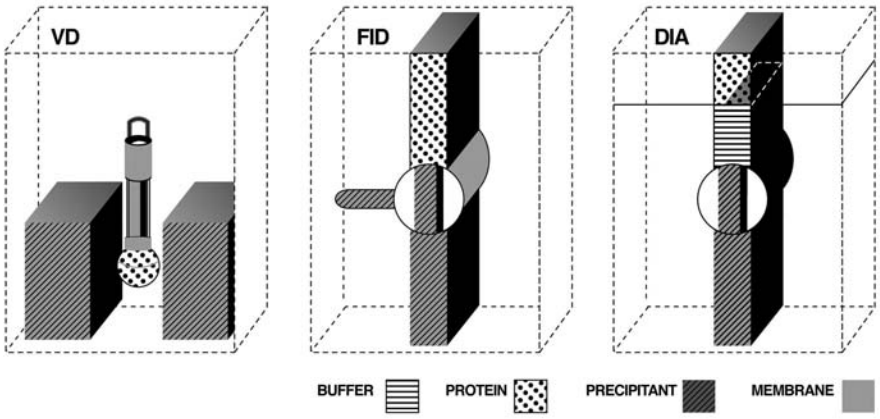

Figure 2
The APCF reactors. Schematic drawing of the VD, FID and DIA reactors showing the protein and precipitant chambers. In FID and DIA reactors, a semi-permeable membrane can be inserted between the chambers. In the VD reactor, the protein solution is contained in a glass cylinder and extruded by a piston upon activation. The DIA and FID reactors are activated by rotating the central cylindrical plug.

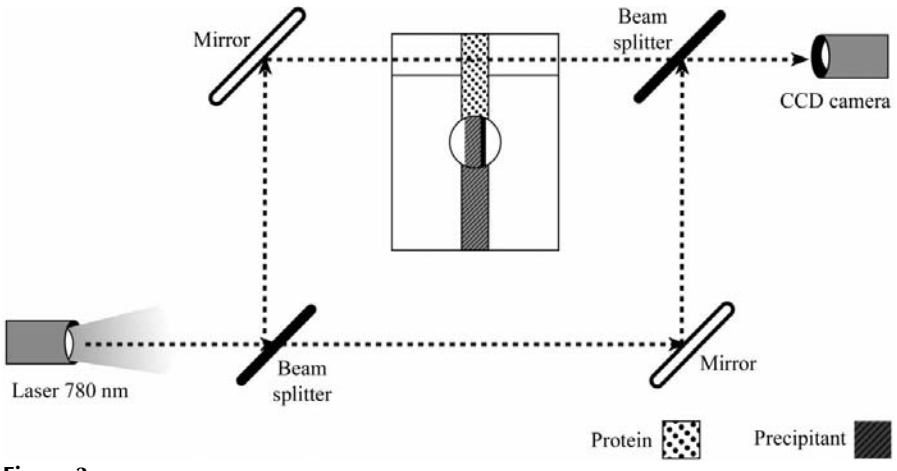

Figure 3
Scheme of the Mach–Zehnder interferometer implemented in the APCF. Details are given in §3.2.

Transport properties in the solutions in which protein crystals grow have been extensively investigated. DLS measures the decay of the autocorrelation function of the electric field of the light scattered by a protein in Brownian motion. By applying a phenomenological relation for the protein diffusion to the characteristic time of this decay, the mutual diffusion coefficients and information about the size distribution in the solution can be obtained. Therefore, DLS has been used to estimate the homogeneity and monodispersity of the sample (Mikol *et al.*, 1990; Dieckmann *et al.*, 1997; Dieckmann & Dierks, 2000), to distinguish crystallization from amorphous precipitation conditions (Kam *et al.*, 1978; Mikol *et al.*, 1990), to follow nucleation and recently to optimize the crystallization outcome (Saridakis & Chayen, 2000; Saridakis *et al.*, 2002). DLS is the most widespread technique for the measurement of diffusion coefficients, even though it is only sensitive to the motion of colloidal particles. A more accurate description of the diffusion process can be achieved using Gouy or Rayleigh interferometry. These methods explicitly consider the multicomponent nature of crystallizing protein solutions, including cross interactions between the protein flow and the concentration gradient of the precipitant (and *vice versa*). From these data, it was possible to extract the derivative of the chemical potential of the protein with respect to the precipitant concentration (and *vice versa*) (Annunziata *et al.*, 2000; Vergara, Paduano *et al.*, 2002). This information is complementary to the second virial coefficient and is linked to the cross driving force of nucleation and of crystal growth. Diffusion coefficients are also important in evaluating the suitability of slow-diffusing precipitants such as high-molecular-weight poly(ethylene glycol) (Vergara *et al.*, 1999) during short space missions or in the case of passive reactors that are not activated by the crew.

Multidimensional phase diagrams (Ducruix & Giegé, 1999) are essential to define the partition of a biological particle among several phases (soluble, crystallized, precipitated *etc.*) at different degrees of supersaturation (Fig. 1). Furthermore, they are important to the analysis of the thermodynamics of crystallization (Riès-Kautt & Ducruix, 1997) and the mechanisms of crystal growth (Zhu *et al.*, 2001). Finally, they are necessary to evaluate the kinetic constant and to serve as an input for numerical simulations (see §3.3).

3.2. Crystal growth

Once the energy barrier has been crossed, critical nuclei can grow. The mechanism by which their growth proceeds depends upon the supersaturation and specific properties of the protein. Growth originating at screw dislocations, growth arising from two-dimensional islands, normal growth (McPherson, 1999) and growth by three-dimensional nucleation (unique to macromolecular crystals and probably arising from liquid protein droplets) have been observed (McPherson *et al.*, 2001). On a macroscopic scale, crystal growth can be monitored using an optical microscope with a resolution of a few micrometres. Time-lapse image recording may be useful to measure growth rates and to observe crystal motion, changes in morphology and in crystal distribution. Video microscopy may be useful to pinpoint crystals to be further investigated by interferometric methods, such as Mach–Zehnder interferometry (MZI) and Michelson interferometry (MI). The latter methods can also be employed to monitor mass transport during crystal growth (Snell, Helliwell, Boggon *et al.*, 1996).

The diagram in Fig. 3 represents the optical setup used for MZI. A fringe pattern that displaces with time results from interference between the beam passing through the protein chamber and the reference beam. The instrument used in the APCF is adjusted to have a minimum initial number of such interference fringes (García-Ruiz *et al.*, 1999). The pattern can be converted into a concentration profile by counting the number of fringes and taking into account the refractive index of the solution as a function of the protein and precipitant concentration. When the precipitant enters the protein chamber, it generates a fringe pattern which becomes stable only once the precipitant concentration is homogeneous. Crystallization is then accompanied by changes in fringe number and position. Therefore, MZI provides information about precipitant transport during nucleation and about the protein-concentration gradient around growing crystals. Further information may be gained from the intensity variation of fringes as a function of time when using a stable light source (Otálora, Novella *et al.*, 1999).

MI and atomic force microscopy (AFM) provide information about crystal growth on a microscopic scale. MI uses slightly different optics to MZI. One of its applications is the accurate determination of the kinetic coefficient for the incorporation of a molecule into a crystal (Chernov *et al.*, 1988). The method is based on the interference of a reference beam with the wavefront of light reflected by a growing crystal face. AFM uses a laser beam to monitor the deflections of a miniature cantilever tip that scans the surface of a crystal in solution (McPherson *et al.*, 2001). Despite the softness of macromolecular crystals, AFM has provided images illustrating the above-mentioned growth mechanisms and has also visualized defects arising from impurities and from fast growth. It was also possible to deduce kinetic and thermodynamic parameters (*e.g.* step free energy and kinetic coefficient of steps) from growth rates as a function of supersaturation or of other chemical physical parameters (Yau *et al.*, 2000).

3.3. Numerical simulation

Thermodynamic, hydrodynamic and kinetic parameters determined with the help of the above physical methods allow prediction of the concentration profiles of protein and precipitant in the crystallization vessel if a correct physical model and an appropriate numerical method are used. Lin *et al.* (1995) performed a complete numerical analysis of crystal growth and Castagnolo *et al.* (2002) extended this analysis by including coupled flows. Lee & Chernov (2002) and Lin *et al.* (2001) numerically estimated that there should be a difference in quality between normal gravity- and μ*g*-grown crystals that

can be ascribed to a greater amount of impurity in the former crystals. The occurrence of convective motion owing to the Marangoni effect was also investigated from a numerical point of view (Savino & Monti, 1996). The step that is the most difficult to describe is nucleation because of the limited experimental data (Galkin & Vekilov, 1999) and valid theories (Dixit *et al.*, 2001).

4. How crystal quality is assessed

Several criteria are generally used to estimate the quality of macromolecular crystals, with morphological and diffraction properties being the most common. Crystal morphology and crystalline defects have been visualized by microscopic methods such as optical, atomic force (McPherson *et al.*, 2001) and electron microscopy (Rodriguez-Fernandez *et al.*, 2002). Frequently, diffraction analyses have been the sole approach used to evaluate the degree of order in protein crystals. On the other hand, biochemical analyses have been used to compare the composition of crystals with that of the initial sample.

4.1. X-ray diffraction analyses

The quality and perfection of biological crystals is commonly evaluated by analyzing the shape, intensity and distribution pattern of Bragg reflections. The order at long distance within a crystal is reflected by the diffraction limit d, linked through the Bragg law to the maximum angle measured for the diffracted beam. The higher the resolution, the higher the crystal order. Small improvements are considered to be relevant because the total number of reflections is roughly equal to $4V/d^3$, where V is the unit-cell volume. Unfortunately, the resolution values reported on several occasions are based on only a few observed intensities and do not correspond to a minimum of 50% of the theoretically measurable reflections in the outer shell having a signal-to-noise ratio $|I|/|\sigma(I)| > 2$, as recommended (Sheldrick, 1990; Dauter *et al.*, 1995). $|I|/|\sigma(I)|$ against resolution also gives information about the diffraction quality. The Wilson plot yields the overall atomic displacement parameter (usually referred to as the thermal factor B). Together, these analyses provide an accurate way to compare space- and earth-grown crystals.

On the other hand, crystal defects can be estimated on the basis of the full-width at half-maximum (FWHM) of the profile of Bragg reflections. The broader the profile, the more the mosaic blocks forming the crystal are misaligned (mosaicity is expressed by the rocking width deconvoluted from geometrical and instrumental effects; it is an angle of a few to a few tens of arcseconds). An ideal protein crystal is assumed to have a theoretical FWHM $\simeq 1''$ (Helliwell, 1988; Fourme *et al.*, 1995; Borgstahl *et al.*, 2001). The lowest experimental values reported so far are $\sim$3–4$''$ for a single block and $\sim$5$''$ for a complete collagenase crystal (prepared on earth). Thus, soft protein crystals may well be assemblies of mosaic blocks that have many defects (Malkin *et al.*, 1996) and for this reason will never reach theoretical perfection (Otálora, Capelle *et al.*, 1999). The presence and distribution of such defects have been visualized on topographs (Stojanoff *et al.*, 1996), which are real-size images displaying regions of high and low contrast (Lorber, Sauter, Robert *et al.*, 1999). Interpretation of the latter can give clues about the nature and origin of defects (Robert *et al.*, 2001). Finally, the ultimate step in comparing the crystallographic quality of crystals prepared under different physical chemical conditions is the straight interpretation of the electron-density maps with the structure models. The anomalous diffraction of S atoms has also been used efficiently as a tool for comparison (Ng *et al.*, 2002).

4.2. Protein analyses

According to a recent hypothesis, the amount of impurity segregated inside crystals grown in μ*g* differs from that of crystals grown on earth (Carter, Lim *et al.*, 1999; Thomas *et al.*, 2000; Chernov *et al.*, 2001; Lorber & Giegé, 2001), although this may not always be the case (Snell *et al.*, 2001). The composition of macromolecular crystals and their mother liquor can be characterized using techniques such as polyacrylamide gel electrophoresis, high-performance liquid chromatography or mass spectrometry. Since most impurities (macromolecules or small molecules) are present as traces, any other analytical method that may selectively detect the contaminant(s) may be applied (*e.g.* protein sequencing, UV or visible light spectrometry, activity assay *etc.*). Finally, another interesting source of information about the crystallization process itself is solubility. It can be determined in the same way as the initial protein concentration (*e.g.* by measuring absorbance, refractive index, fluorescence or any other physicochemical property).

5. Results from experimentation with the APCF

The APCF went into space for the first time aboard a space shuttle orbiter in June 1993, 10 y after the first protein crystallization experiment in μ*g* (Littke & John, 1984). Since then it has flown five more times. In the following, the term 'protein' will refer in a somewhat inaccurate way to all types of biological particles, including proteins, RNA and DNA molecules as well as nucleo-protein complexes and assemblages such as nucleosomes, ribosomes and viruses. The term microgravity (μ*g*) will stand for any level of reduced gravity encountered in space. Table 1 lists the missions on which biological particles have been crystallized in μ*g* with this facility and Table 2 gives details of the proteins ranked by size. Including the ISS-3 mission that took place from August to December 2001, a total of 474 samples representing 50 different proteins have been crystallized (this includes all crystal forms and protein mutants).

5.1. Hydrodynamics

Mass transport occurring in crystallizing protein solutions has been well characterized. Firstly, mutual diffusion coefficients measured by Gouy and Rayleigh interferometry in the absence of crystals (Albright *et al.*, 1999; Annunziata *et al.*, 2000; Vergara, Paduano *et al.*, 2002) have led to predictive

Table 2
Proteins crystallized with APCF and related references.

The symbols in the Result column are: +, the structure from space-grown crystals has been solved and published; /, crystals diffracted better but the data collection was not complete; =, crystal showed equal diffraction properties to earth-grown crystals; −, crystals were not suitable for diffraction analysis, similar to earth-grown crystals; w, space-grown crystals exhibited poorer diffractive properties than earth control crystals.

Biological particles	MW† (kDa)	Missions‡	Result	References§
Small				
$(Pro\text{-}Pro\text{-}Gly)_{10}$	8	E, F	+	Berisio *et al.* (2000, 2001); Berisio, Vitagliano, Mazzarella *et al.* (2002); Carotenuto *et al.* (1999, 2000, 2001*a*,*b*); Berisio, Vitagliano, Vergara *et al.* (2002); Vergara, Corvino *et al.* (2002)
5S rRNA domains	8	B–D, F	/+¶	Lorenz *et al.* (2000); Vallazza *et al.* (2001, 2002)
Topoisomerase poison, CcdB	12	C, D	/	Dao-Thi *et al.* (1998); Loris *et al.* (1999).
Lysozyme (avian), tetragonal form	14	A–F	+	García-Ruiz & Otálora (1997); Otálora & García-Ruiz (1997); Riès-Kautt *et al.* (1997); Broutin *et al.* (1997); Vaney *et al.* (1996); Snell *et al.* (1995); Stojanoff *et al.* (1996); Otálora *et al.* (1999, 2001); Otálora, Novella *et al.* (1999); Dong *et al.* (1999); Sauter *et al.* (2001); García-Ruiz *et al.* (2001); McPherson (1997); Snell (1997)
Lysozyme (avian), triclinic and monoclinic form	14	C	+	Vaney *et al.* (2001).
Ribonuclease A	16	A	−	
Ribonuclease S	16	B	/	
Lysozyme (viral)	17	C	−	
Antigen–antibody complex	17	E, F	+	Decanniere *et al.* (2001); Zegers *et al.* (2002)
Apocrustacyanin C1	20	B–D	/	Chayen *et al.* (1996, 1997); Snell *et al.* (1997); Dieckmann *et al.* (1997); Snell (1997); Stojanoff *et al.* (1996)
Adaptor Grb2	*20*	E	−	
Epidermal growth-factor receptor	*20*	C, D	=	
Thaumatin	22	B–F	+	Lorber *et al.* (1999*b*); Ng *et al.* (1997, 2002); Lorber & Giegé (2001); Lorber *et al.* (1999*a*, 2000); Lorber, Sauter, Robert *et al.* (1999); McPherson (1997); Sauter *et al.* (2002); Théobald-Dietrich *et al.* (2001)
Rhodopsin (bacterial)	25	A, B, D, E	/	Wagner (1993, 1994, 1996); Wagner & Rotharmel (1996); Wagner *et al.* (1995); Zorb *et al.* (2002)
Collagenase	25	B	+	Broutin *et al.* (1997); Broutin-L'Hermite *et al.* (2000)
Medium				
Octarellin II	28	B, C, E, F	/	
Octarellin III	28	B, C, E, F	−	
Concanavalin B	37	C	−	
5S rRNA	40	B–E	/	Barciszewska *et al.* (2000); Lorenz *et al.* (2000)
Rhodopsin (bovine)	40	A–C, F	−	
Proteinase K	45	E	+	Betzel *et al.* (2001); Eschenburg *et al.* (2000)
Antithrombin	50	E	−	
Glutathione S-transferase	50	C	−	
Single-strand DNA-binding protein ssDNA	60	E	−	Mapelli & Tucker (1999)
Triose P isomerase (human)	75	B, C	−	
Triose P isomerase (human, mutant)	75	B, C	/	
Triose P isomerase (*Thermatoga*)	75	B, C	w	
Outer surface glycoprotein	76	E	/	Evrard *et al.* (1999).
Aspartyl-tRNA synthetase	132	B–F	+	Lorber *et al.* (1999*b*); Ng *et al.* (1997, 2002); Théobald-Dietrich *et al.* (2001)
Canavalin, hexagonal form	142	B, C	+	Ko *et al.* (2000); Koszelak *et al.* (1995)
Canavalin, rhombohedral form	142	B, C	+	Ko *et al.* (2001)
Phenyl-tRNA synthetase	*150*	E	−	
Alcohol dehydrogenase	150	C, D	/	Carotenuto *et al.* (1997); Esposito *et al.* (1997, 1998)
Large				
Photoreactor center	*200*	B	w	
Nucleosome	206	D	=	
Catalase	240	C	/	McPherson (1996).
Apoferritin	450	C, E	=	Otálora & Vidal (1998).
Ferritin	474	E, F	/	Otálora *et al.* (2001); Otálora & Vidal (1998)
Low-density lipoprotein particle	550	F	−	
Lumazine synthase	1000	F	=	Rodriguez-Fernandez *et al.* (2002)
Photosystem I	1020	C–E	+	Klukas *et al.* (1999*a*,*b*); Laubender *et al.* (2002)
Satellite panicum mosaic virus	1200	B, C	−	Koszelak *et al.* (1995)
Satellite tobacco mosaic virus, cubic form	1400	B, C	/	Koszelak *et al.* (1995); Kuznetsov *et al.* (2001); McPherson (1996)
Tomato aspermy virus	*2000*	C	−	
Ribosome	2300	B,C	−	
Turnip yellow mosaic virus	5600	B, C	−	Koszelak *et al.* (1995)

† Proteins are divided in three classes: small (MW < 25 kDa), medium (25 < MW < 200 kDa) and large (MW > 200 kDa). Approximate molecular weights are given in italics when this information could not be found in publications. ‡ Letters refer to different space missions: A, B, C, D, E and F stand for SpaceHab-01, IML-2, USML-2, LMS, STS-95 and ISS-3, respectively. § When no reference is listed, see NASA report or ESA Microgravity Database for available information. ¶ The crystal structure is forthcoming.

equations (Vergara *et al.*, 2000). Secondly, mass transport in the presence of crystals could be followed by Mach–Zehnder interferometry on earth as well as in μ*g* (Snell, Helliwell, Boggon *et al.*, 1996; García-Ruiz *et al.*, 1999; McPherson *et al.*, 1999; Otálora *et al.*, 2001; García-Ruiz, Otálora *et al.*, 2001). Finally, numerical simulations were applied to predict the time evolution of the protein-concentration profile (Lin *et al.*, 1995; Cang & Bi, 1999, 2001; Castagnolo *et al.*, 2001, 2002; Lin *et al.*, 2001) and to interpret Mach–Zehnder interferograms (García-Ruiz *et al.*, 1999; Otálora, Novella *et al.*, 1999; Otálora *et al.*, 2001).

5.2. Crystal nucleation

Homogeneous nucleation occurs in the bulk of the solution. In contrast, heterogeneous nucleation occurs on solid surfaces such as reactor walls or membranes, requiring a lower activation energy. Video observation during the APCF mission was very useful for examining the crystallization behaviour in various types of reactors (VD, FID, DIA) and media (solution or gelled) in different environments (1*g* or μ*g*) (see §5.3). It revealed that the results may differ significantly (García-Ruiz & Otálora, 1997; Lorber *et al.*, 2000; Lorber & Giegé, 2001; Vergara, Corvino *et al.*, 2002).

If FID and DIA reactors behave as real counter-diffusion reactors, the time of appearance of the first crystals should be correlated to the distance between them and the initial boundary/membrane. Video observation (García-Ruiz & Otálora, 1997; Lorber *et al.*, 2000; Carotenuto *et al.*, 2001*b*; Vergara, Corvino *et al.*, 2002) and numerical simulations (Otálora & García-Ruiz, 1997) indicate that the nucleation probability inside these APCF reactors is uniform and that they hence actually behave like BAT reactors. This is the reason why some experimenters have suggested modifying reactors to have longer protein chambers. Such reactors (named XL-FID) were manufactured and the benefits of counter-diffusion, such as the self-screening of optimal conditions, could thus be proved experimentally (García-Ruiz & Otálora, 1997; Otálora, Novella *et al.*, 1999).

Nucleation is a process occurring far from equilibrium and large differences in lag time owing to slight differences in local conditions within a single reactor can reasonably be expected. This may explain the broad range of lag time that was observed (Lorber *et al.*, 2000; Lorber & Giegé, 2001). Furthermore, nucleation times (Lorber & Giegé, 2001) and the required supersaturation (Lorber *et al.*, 2000; Lorber & Giegé, 2001) have been occasionally reported to be different in the two gravity environments. In some cases, no difference was found (Riès-Kautt *et al.*, 1997). Conversely, the lag time is markedly reduced in gel (Lorber & Giegé, 2001), suggesting that a more uniform environment is created inside the micrometric pores of the matrix (Lorber, Sauter, Robert *et al.*, 1999), even though in other cases no differences were observed (Vergara, Corvino *et al.*, 2002).

5.3. Crystal motion in μ*g* environments

In an orbiting spacecraft or space station, the μ*g* environment is not ideally quiescent (Snell, Boggon *et al.*, 1997). Indeed, residual acceleration with frequency f and modulus a was recorded on most shuttle flights. Accelerometer data are publicly available on the NASA website. According to a classification by Kundrot *et al.* (2001), acceleration is either quasi-steady (f = 0.01 Hz, a = 0.1–0.3μ*g*), oscillatory (*g*-jitter with 0.01 Hz < f < 300 Hz) or transient (with spikes as high as 0.1*g*). Each mission is characterized by its own acceleration profile, with fluctuations in frequency and amplitude. Furthermore, minor local differences may be present inside the orbiter. Video images recorded at regular time intervals over the entire duration of several missions clearly show that crystals seldom nucleate or grow in a steady solution (Lorber *et al.*, 2000). Often, disturbances in the gravity level trigger the displacement of the crystals (the effect may be amplified for larger and thus heavier crystals). Once the latter are in motion, their trajectories may be of several kinds as displayed in Fig. 4. Motion is either an individual or a collective phenomenon. It can be either coherent (when the crystals move in the same direction) or incoherent and synchronous (when crystals move at the same time) or asynchronous (*e.g.* Lorber *et al.*, 2000). A

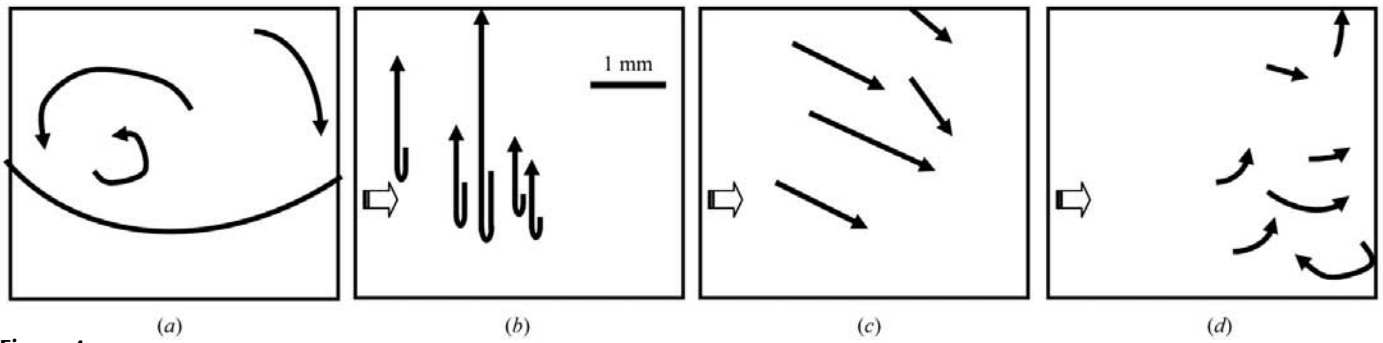

Figure 4
Crystal motion observed inside APCF reactors. References for the experimental data are: (*a*) crustacyanin A crystal motion owing to Marangoni convection in a VD reactor on the IML-2 mission (Chayen *et al.*, 1997), causing fast mixing; (*b*) synchronous and coherent motion of $(Pro\text{-}Pro\text{-}Gly)_{10}$ crystals in a DIA reactor on the ISS-3 mission (Vergara, Corvino *et al.*, 2002); (*c*) synchronous but incoherent motion of thaumatin crystals in a FID reactor on the USML-2 mission (Lorber *et al.*, 2000); asynchronous and incoherent motion of thaumatin crystals in a DIA reactor on the LMS mission (Lorber *et al.*, 2000). The arrow on the left-hand side in the FID and DIA reactors indicates the entry of the precipitant. Crystal motion was totally suppressed in agarose gel.

Table 3
Percentage of nucleation probability in the bulk for thaumatin and (Pro-Pro-Gly)$_{10}$ crystals in different environments (solution on ground and in μ*g*, gel on ground and in μ*g*).

Protein	Earth (%)	μg (%)	References
Thaumatin			
Solution	0	29 ± 12	Lorber *et al.* (2000).
Gel	49 ± 30	83 ± 2	Lorber & Giegé (2001).
(Pro-Pro-Gly)$_{10}$			
Solution	0	15 ± 10	Carotenuto *et al.* (2001*a*,*b*); Vergara, Corvino *et al.* (2002).
Gel	50 ± 15	75 ± 8	Vergara, Corvino *et al.* (2002).

correlation between crystal movements, fluctuations in growth rate and crystal quality was found (García-Ruiz & Otálora, 1997; Snell, Boggon *et al.*, 1997; Boggon *et al.*, 1998). The most rapid motion observed in VD experiments was attributed to Marangoni convection, *i.e.* flow induced by changes in surface tension at solution–vapour interfaces (Chayen *et al.*, 1997). It has even been correlated with differences in quality between crystals prepared by VD and by FID or DIA techniques (Esposito *et al.*, 1998), although good results were obtained by using a vapour-diffusion-based apparatus, as in the PCAM facility (Carter, Wright *et al.*, 1999). The APCF result may seem to be in contradiction with the fact that forced flow may improve crystal quality (Vekilov *et al.*, 1996) (see §5.4). For this reason, the VD technique was abandoned after the STS-95 mission. Furthermore, despite being widespread, this technique is now considered to have been one of the causes of the low success rate of early space crystallization experiments (Chayen & Helliwell, 1999). The lesson to be learnt is that fluctuations in residual acceleration should be kept minimal for better reproducibility of crystallization results. Unfortunately, because of crew activity and vibrations generated by equipment and instruments, the level of μ*g* on manned orbiters will never be as low and stable as on unmanned satellites (Boggon *et al.*, 1998). Appropriate isolation of the crystallization facility should help to attenuate at least some vibrations (Kundrot *et al.*, 2001).

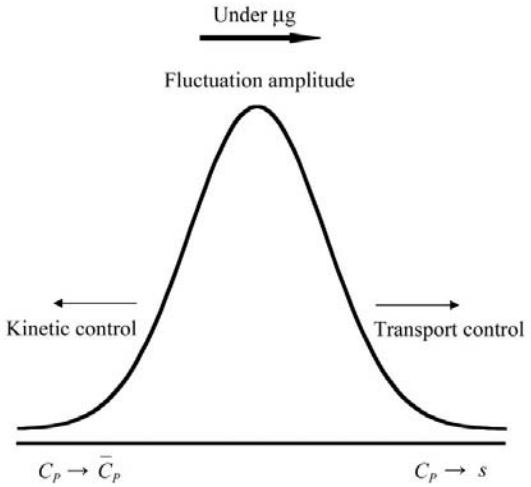

Figure 5
Dependence of the kinetic fluctuation amplitude on the coupling between transport and interface processes (after Vekilov *et al.*, 1996). Crystallization is essentially controlled by the incorporation kinetics of molecules in the crystals at high supersaturation (*e.g.* when protein concentration C_P around the crystals approaches the concentration in the bulk, $\bar{C}_P$). It is controlled by transport at low supersaturation (*e.g.* when protein concentration C_P around the crystals approaches solubility s).

The combination of nucleation probability and crystal trajectory determines the final crystal distribution (Carotenuto *et al.*, 1999, 2001*a*,*b*; Vergara, Corvino *et al.*, 2002). Because of the absence of sedimentation, the crystal distribution depends on where crystals grow (see §5.2) and how they move (considering that larger crystals move faster than smaller ones according to Stokes theory) (Kundrot *et al.*, 2001). Table 3 summarizes the results for thaumatin and (Pro-Pro-Gly)$_{10}$. For both molecules, heterogeneous nucleation on the walls of the protein chamber is significantly reduced in solution in μ*g* (as also observed by Wagner, 1994) and the effect is even stronger in agarose gel. This property, plus the protection of the crystals from mechanical shocks and from thermal fluctuations, should urge investigators to also test the effect of gels under reduced gravity (Lorber *et al.*, 1998; Lorber, Sauter, Robert *et al.*, 1999; Lorber & Giegé, 2001; Sauter *et al.*, 2002; Vergara, Corvino *et al.*, 2002).

5.4. Crystal growth and rates

The existence of concentration-depletion zones (CDZ) around growing crystals was predicted based on theoretical considerations (McPherson, 1993) and on numerical simulation (Grant & Saville, 1991 and references therein; Lin *et al.*, 1995). Such zones were first observed on earth as 'haloes' in optical microscopy (Kam *et al.*, 1978; Chayen *et al.*, 1997) and also with MI (Miyashita *et al.*, 1994) and MZI (McPherson *et al.*, 1999). Later, they were visualized by MZI under μ*g* (Otálora *et al.*, 2001). Interestingly, CDZs are more stable under μ*g* or in gel than in solution under 1*g* (Otálora *et al.*, 2001). Thus, there is a lower local supersaturation around each growing crystal, but the resulting reduction in supersaturation was recently evaluated from theoretical studies to be negligible (Lee & Chernov, 2002).

Measurements of crystal-growth rates (R) (García-Ruiz & Otálora, 1997; Otálora & García-Ruiz, 1997; Carotenuto *et al.*, 1997, 1999, 2000, 2001*a*,*b*; Chayen *et al.*, 1997; Riès-Kautt *et al.*, 1997; Snell, Boggon *et al.*, 1997; Otálora, Novella *et al.*, 1999; Lorber *et al.*, 2000; Lorber & Giegé, 2001; Vergara *et al.*, 2001; Vergara, Corvino *et al.*, 2002) at different relative supersaturations s enables testing of the theory of the growth mechanism and evaluation of the face kinetic constant β_0 from $R = \beta_0\sigma^n$ (Ducruix & Giegé, 1999) (with the exponent n being related to the mechanism of growth and with $\sigma = \ln s$). So far, kinetic parameters are available for only a few proteins (Vekilov *et al.*, 1996).

Although the absence of sedimentation and segregation of impurities are unanimously considered to be features that are favourable when crystallization takes place in μ*g*, theory predicts that the effect of a reduction of the transport rate is system-dependent. It may be either an advantage or a disadvantage (Vekilov *et al.*, 1996). Large fluctuations (by as much as 80%) in growth rate, vicinal slope and tangential

Table 4
Major results from APCF experimentation in reduced-gravity environment *versus* on earth.

	Trends in μ*g*
Crystallogenesis	Diffusional self-purification of the macromolecule incorporating in crystals
	High nucleation probability in the bulk
	Stable protein-depleted zone around growing crystals
	Equidistance between each crystal and its closest neighbours
Properties of μ*g*- *versus* ground-grown crystals†	Better morphologies (67%)
	Larger dimensions and volume (65%)
	Higher diffraction limits (52%) yielding more accurate structures (26%)
	Lower mosaicities (57%); never higher
	Reduced packing defects, such as twinning (50%)

† The percentages refers to the number of proteins possessing the specific feature compared with the total number of proteins.

velocity originating from coupling of bulk transport with nonlinear interface kinetics (see Fig. 5) have been numerically predicted and experimentally observed (Vekilov & Rosenberger, 1998). The step-bunch kinetics causing striations in crystals is governed by the kinetic Peclet number (Pe_k), a system-dependent parameter measuring the relative weight of bulk transport and interface kinetics. Authors have argued that under either pure kinetic or transport control, any perturbation may decay and hence crystal quality may be improved. On the contrary, in a mixed kinetic–bulk system, crystal quality is expected to be poorer under μ*g* (Vekilov & Rosenberger, 1998). In short, the gravity effect depends on whether the operating point is located before or after the critical point at which fluctuation amplitude is maximal in Fig. 5. This theory partially predicts the effect of μ*g*: for satellite tobacco mosaic virus and canavalin the quality of the crystals should be improved, whereas for lysozyme and thaumatin it should be unchanged or worse (conversely, a forced flow is expected to produce the reverse effect). In cases where the theoretical results do not match the experimental ones, the authors invoke the benefit of slower diffusing impurities or sedimentation. Although this may not explain all experimental data, it seems important to evaluate whether a growth rate is controlled by kinetic or by transport properties. According to a linear-stability analysis (Chernov & Nishinaga, 1987), Pe_k can be estimated from $Pe_k = \beta_0\delta/D$, where D and δ represent the protein diffusion coefficients and a characteristic diffusion length (commensurate with crystal size), respectively. Since the experimental determination of β_0 is time-consuming, a graph of crystal size aginst time (García-Ruiz & Otálora, 1997; Lorber *et al.*, 2000; Otálora, Novella *et al.*, 1999; Vergara, Corvino *et al.*, 2002) or the comparison of the growth rate in different crystallization environments have been used to obtain qualitative information on the growth-rate control (Lorber, Sauter, Robert *et al.*, 1999; Vergara, Corvino *et al.*, 2002).

Another nonlinear process that characterizes complex phenomena (such as protein crystallization) has been observed in the form of supersaturation waves. This was the case during lysozyme crystallization in gel on earth and under μ*g* (García-Ruiz, Otálora *et al.*, 2001). Such waves are formed in the case of protein crystals and differ from the rings arising from the presence of negligible precipitant concentration inside the protein crystals. They also differ from the annular zones known as Liesegang rings which occur during the crystallization of inorganic salts where the precipitant has a common ion with the precipitate (Henisch, 1988).

It is noteworthy that in some experiments crystal growth was not complete at the end of the μ*g* session (Carotenuto *et al.*, 2001*b*; Lorber & Giegé, 2001) and that crystals nucleated under μ*g* may have served as seeds for growth on earth. This event was corrected by a longer mission duration, as provided on the ISS where crystal growth was actually monitored until cessation (Vergara, Corvino *et al.*, 2002; Lorber *et al.*, unpublished data). Nevertheless, experimenters should be aware of the fact that crystal quality is best at the end of growth and that it may be altered by crystal ageing (Berisio, Vitagliano, Vergara *et al.*, 2002).

5.5. Diffraction properties of space- *versus* earth-grown crystals

The first evidence that protein crystallization benefits from μ*g* was provided by the better morphology and larger size of crystals (Table 4). Crystals with smaller dimensions have rarely been observed (this has only actually been mentioned in the reports of space agencies and has never been published elsewhere). How the diffraction limit of these better-looking crystals is influenced by μ*g* will be discussed in §6.2 after a statistical analysis of the data. Values of intensity-to-sigma ratios as a function of resolution have frequently been reported to be superior for μ*g*-grown crystals. Only in a few cases were they equal or inferior (Table 2). The same trend was reported for atomic displacement parameters, which are usually greater for earth-grown crystals (Table 2). Mosaicity, *i.e.* the degree of misalignment of the microscopic blocks forming the crystal, was either reduced (Snell *et al.*, 1995; Snell, Helliwell, Cassetta *et al.*, 1996; Snell, 1997; Snell, Cassetta, Helliwell *et al.*, 1997; Ng *et al.*, 1997; Lorber *et al.*, 1998; Otálora, Capelle *et al.*, 1999) or unchanged. Crystal twinning was reported to be reduced in some cases (Dao-Thi *et al.*, 1998; Esposito *et al.*, 1998).

The effect of impurities as a discriminant between the quality of earth and μ*g* protein crystals has been experimentally investigated (Carter *et al.*, 1999; Thomas *et al.*, 2000; Chernov *et al.*, 2001; Lorber & Giegé, 2001; Snell *et al.*, 2001). A numerical simulation (Lin *et al.*, 2001) put forward the hypothesis that under μ*g* a 'diffusional filtration' could segregate impurities in the solution and reduce their incorporation into the crystals (Lee & Chernov, 2002). The relation between growth rate and crystal quality has been experimentally tested (García-Ruiz & Otálora, 1997; Lorber *et al.*, 2000; Otálora *et al.*, 2001) and theory suggests a positive effect of μ*g* if sufficiently long reactors are used (Chernov, 1997; Vekilov & Alexander, 2000). Details of the improved three-dimensional structure models that could be refined using

X-ray data from crystals grown in the APCF will be reported elsewhere.

5.6. Implementation of novel techniques on earth and in space

After the maiden flight of the APCF, a few changes were made to optimize the operation of the reactors (Riès-Kautt *et al.*, 1997). The diameter of the bore of DIA and FID reactors was enlarged to prevent small air bubbles from perturbing the equilibration between the contents of the precipitant and protein chambers. Afterwards, the VD technique was abandoned because convectional currents generated at the vapour–solution interface stir the content of the drops and also because optical imaging is difficult. In parallel, thanks to the combination of results from experiments in space and in earth-based laboratories, investigators have developed new crystallization techniques and setups that are now available to crystal growers. The gel-acupuncture technique, developed for protein crystallization under normal gravity (García-Ruiz *et al.*, 1993), was adapted for use under μ*g*. A device named the Granada Crystallisation Box has been commercialized. A set of containerless techniques where the protein volume is kept under oil are commercially available and a technique that uncouples nucleation from growth has been proposed (Saridakis & Chayen, 2000; Chayen, 2002). Another containerless technique using two immiscible silicone oils has been implemented (Lorber & Giegé, 1996; Chayen, 1997) and commercialized. In parallel to experimentation in low gravity, old crystallization techniques have been rediscovered. In particular, gels have been used as media to simulate μ*g* at least in part. Gels, such as the polysaccharide agarose, have many advantages even under microgravity. It was shown that crystals grown on earth in this gel are of intermediate quality (with regard to their diffraction properties) between crystals prepared in solution on earth and those prepared under μ*g* (Miller *et al.*, 1992; Dong *et al.*, 1999; Lorber, Sauter, Robert *et al.*, 1999). Agarose gel was used to suppress crystal motion under μ*g* and to prevent crystals from settling upon their return to gravity (Lorber & Giegé, 2001). It helped to preserve the optical and the diffraction properties of thaumatin crystals (Lorber, Sauter, Robert *et al.*, 1999; Sauter *et al.*, 2002). Despite these advantages, experimenters should be aware that specific interactions occurring between the gel matrix and some proteins may affect the solubility and the nucleation (Thiessen, 1994; Vidal *et al.*, 1996, 1998). Accordingly, μ*g* has been termed a 'clean' gel (Robert *et al.*, 1999).

6. General discussion

6.1. Beneficial effects of reduced gravity

Thanks to NASA and to negotiations with ESA and other national space agencies, the unique low-gravity environment generated by space missions was offered to the international crystal-growth community. The benefit was that various aspects of the physical chemistry of protein crystal growth that had never previously been studied could be investigated. The major result is the demonstration that transport mechanism and sedimentation do have an effect on protein crystal growth and crystal quality. Table 4 summarizes the positive effects on crystallogenesis and on crystal quality found so far with the APCF. The stability of the protein-depleted zones forming as crystals grow and the diffusional transport are major differences between the crystallization process in μ*g* and on earth.

Better morphology, larger volume and higher order distinguish the crystals grown in μ*g* from those prepared on earth. Another common point, reduced mosaicity, also confirmed by crystals grown within other facilities (Yoon *et al.*, 2001), suggests a reduction in the crystal defect density arising from the reduced flow velocity in μ*g*. When compared with earth-based experiments, the nucleation in μ*g* seems to be more homogeneous, eventually proceeding at a different rate and resulting in more equidistant crystals. Although crystal sedimentation is almost absent, crystal motion can be caused by residual acceleration. Motion can be avoided by using a gel or by attenuating vibrations in appropriate isolation systems. Finally, the higher homogeneity of nucleation probability and the absence of crystal motion result in a more uniform crystal distribution.

6.2. The contribution of the APCF

So far about 100 publications have appeared reporting results obtained with the APCF. Half of them essentially deal with protein crystallogenesis and the others with crystal quality and structural determination. Statistics (based on data in Table 2) indicate that the crystals of 26% of the proteins assayed in the APCF under μ*g* had better diffraction properties than any previously earth-grown crystal. Furthermore, this percentage corresponds to crystals that were suitable for complete data collection and structural determination and that led to the publication of a three-dimensional structure model. The success rate increases to 52% when crystals which diffracted to a higher resolution than any earth-grown crystal but were not sufficiently stable for complete data collection (because of radiation damage owing to the lack of appropriate cryoconditions, twinning *etc.*) were included (Esposito *et al.*, 1998; Evrard *et al.*, 1999; Lorenz *et al.*, 2000). Consequently, this last value represents the potential level of success for the APCF working under reduced gravity. The percentage dramatically increases with the number of missions: it is 29% for proteins that were assayed only once, rising to 65% for those assayed twice and 78% for those assayed three times or more.

Is there any correlation between the rate of success and any system-dependent physicochemical parameter? Since the Pe_k number for most proteins is not known, molecular size was considered because it is inversely proportional to the diffusion coefficient. The trend decreases with size: it falls from 73% for small proteins to 50% for medium ones and to 30% for the largest. This seems to be in disagreement with the prediction of the nonlinear response theory (Vekilov & Alexander, 2000). Therefore, it would be interesting to extend this analysis to the complete set of proteins that have been crystallized on

Table 5
Recommendations for improving macromolecular crystallization and minimal crystallogenesis investigation with the APCF to compare the effect of μg *versus* normal gravity and of crystal growth in solution *versus* gel.

Use	Purest biological sample
	Extensive ground research to optimize crystallization (solubility, two-dimensional phase diagram)
	Controlled protocols for parallel experiments under μg and 1*g*
	Equilibration by DIA or FID rather than by VD
	Low precipitant-concentration gradients in FID and DIA
	Addition of gel to suppress crystal sedimentation or motion
Compare by	
Video-image analysis	Nucleation probabilities *versus* time and position
	Crystal-growth rates
	Crystal sizes *versus* $(\text{time})^{1/2}$
	Morphologies and spatial distributions of crystals
Mach–Zehnder interferometry analysis	Concentration profiles around growing crystals
	Velocity fields around growing crystals
Crystallographic post-flight analysis	Diffraction limits, $I/\sigma(I)$ and Wilson plots
	Electron-density maps and three-dimensional structure model
	Mosaicity and nature and distribution of defects in crystals
Biochemical post-flight analysis	Macromolecular composition and solubility
	Impurity content
	Others

all facilities under μ*g*. As expected, no correlation seems to exist with the isoelectric point. On the other hand, for the APCF there is a strong increase of the rate of success with chronology, in agreement with findings from other experiments carried out in space (Kundrot *et al.*, 2001). However, the gradual improvements in X-ray technology and crystallographic methods should be also taken into account (Kleywegt & Jones, 2002). Promising results have appeared from the ISS-3 mission (Berisio, Vitagliano, Vergara *et al.*, 2002; Vallazza *et al.*, 2002) and others are forthcoming (Rodriguez-Fernandez *et al.*, 2002; Zegers *et al.*, 2002).

Finally, the applications of the APCF are not limited to studies of the physicochemical aspects of protein crystallogenesis. The APCF was used on six space missions out of about 50 that have carried protein crystallization facilities. To date, it has contributed 14 structure models, representing around 40% of the total number of proteins crystallized under μ*g* for which atomic coordinates have been deposited in the Protein Data Bank (Lorber, 2002). Thus, 40% of the structures that were refined using data from crystals grown in space come from only 5% of experiments that were set up with the APCF (5% meaning 474 out of about 10 000 samples crystallized under μ*g*) (Kundrot *et al.*, 2001; Riès-Kautt, 2001).

6.3. Experimental results *versus* theory

The physical reason for better crystal quality may be a consequence of several factors, as discussed below. In space, crystals grow in a more stable medium (as verified by interferometric analyses performed with the APCF), in which variations in local supersaturation are small, possibly yielding fewer defects in the crystal. Theoretically, this reduction in supersaturation does not seem to be large enough to have a major effect. The coupling of nonlinear crystal kinetics and transport can create unfavourable fluctuations in growth rate, which are reduced only for those proteins with a growth rate controlled by transport. Our statistical analysis based on about 50 proteins investigated with the APCF seems to contradict this prediction, even though a more extended sample will be required to verify this statement (as the whole set of proteins were crystallized in μ*g*). The hypothesized positive effect for protein crystals with a higher solvent content has been contradictorily discussed (Dong *et al.*, 1998; Sauter *et al.*, 2002). The major factor might possibly be the diffusional purification induced by the reduced incorporation of impurity into the crystal as a consequence of the impurity depletion zone. This is supported by some observations made during investigations with the APCF; however, the issue of the impurity content in μ*g*-grown crystals is still an open question.

6.4. Recommendations for future experimentation in space

The lessons learnt from crystallizing proteins under reduced gravity and in parallel under normal gravity cover different aspects. Table 5 lists recommendations that should help to further increase the rate of success of future crystallization experiments in the APCF and/or in other facilities. Each point is important, from preparation of the biological sample to knowledge of its properties in solution, from crystallization in solution to that in other media. Also, analyses should be performed on a great number of crystals in order to obtain a significant sampling (Lorber, Sauter, Robert *et al.*, 1999). Therefore, it is advisable that all details of the preparation of the samples and of the crystals, as well as of the analysis protocols, be described not only for space-grown crystals but also for earth-grown controls (Lorber, 2001). Standard protocols for the assessment of the crystal quality should be thoroughly defined. Also, the atomic coordinates (http://www.rcsb.org/pdb/), accelerograms (http://pims.grc.nasa.gov), crystallization protocols, video images and interferograms should be available to the scientific community for further exploitation. This would allow scientists in all fields to have access to them at any time.

7. Conclusion and perspectives

The APCF is a user-friendly and reliable facility that accommodates a reasonable number (48) of reactors. It is flexible because it operates with various types of reactors covering a wide range of sample volumes. Moreover, crystallization can be monitored using various techniques. During these investigations, one *sine qua non* condition was that for each mission sufficient reactors were available to perform control experiments in the laboratory before and in parallel with experiments in orbit. Until now, this facility has provided a wealth of results (i) with respect to the physical chemistry aspects –

nucleation occurs preferentially in the bulk, crystals are surrounded by stable protein-depleted zone and grow equidistant – and (ii) with respect to the crystal properties – the common features are improved morphology, larger volume, higher diffraction limit and lower mosaicity.

Experiments requiring μ*g* sessions longer than those available on the shuttle may now be performed on the ISS. In the long term, an X-ray facility (DeLucas *et al.*, 2002), telescience and robotics (DeLucas, 2001) could enable experimenters to control crystallization conditions remotely. The PCDF (Pletser *et al.*, 1999, 2001*a*,*b*), an upgraded APCF accommodating 11–12 reactors (four batch, four extended DIA and three or four DIA reactors) is planned to reside permanently on the ISS. The following diagnostic methods should be operational: (*a*) high-resolution video-image acquisition through a microscope, (*b*) dynamic light back-scattering and (*c*) MZI or a DLS at 90° angle. All reactors would be monitored by the techniques (*a*) to (*c*), except for extended DIA reactors for the last technique (Pletser *et al.*, *a*,*b*). Although this new facility is supposed to be essentially dedicated to the study of the physics of crystallization, it will not be a substitute for the APCF. In fact, it is equipped with more diagnostics, but it accommodates a smaller number of reactors.

Earth-based crystallization experiments destined to quantify the effects of physicochemical parameters will benefit both space and earth science. More frequent missions in space should enable the crystal-growth community to expand the applications of microgravity-grown crystals of proteins and of other biological macromolecules.[1]

The authors thank Drs Ch. Betzel, N. Chayen, J.-M. García-Ruiz, J. Helliwell, M. Riès-Kautt, C. van de Weerdt and G. Wagner for their help in collecting information, Drs O. Minster and P. Di Palermo (ESA) for use of the APCF, NASA for flight opportunities, and Drs R. Bosch, L. Potthast, J. Stapelmann and P. Lautenschlager (Astrium GmbH) for their assistance. AV and AZ acknowledge the Italian Space Agency (ASI), and BL and RG acknowledge CNES for financial support. AV also acknowledges the University of Naples 'Federico II' for a fellowship.

References

Asterisks indicate articles containing results obtained with the APCF.

Albright, J. G., Annunziata, O., Miller, D. G., Paduano, L. & Pearlstein, J. (1999). *J. Am. Chem. Soc.* **121**, 3256–3266.

Annunziata, O., Paduano, L., Pearlstein, J., Miller, D. G. & Albright, J. G. (2000). *J. Am. Chem. Soc.* **122**, 5916–5928.

Barciszewska, M. Z., Szymanski, M., Erdmann, V. A. & Barciszewski, J. (2000). *Biomacromolecules*, **1**, 297–302.*

Berisio, R., Vitagliano, L., Mazzarella, L. & Zagari, A. (2001). *Biopolymers*, **56**, 8–13.

Berisio, R., Vitagliano, L., Mazzarella, L. & Zagari, A. (2002). *Protein Sci.* **11**, 262–270.*

Berisio, R., Vitagliano, L., Sorrentino, G., Carotenuto, L., Piccolo, C., Mazzarella, L. & Zagari, A. (2000). *Acta Cryst.* D**56**, 55–61.*

Berisio, R., Vitagliano, L., Vergara, A., Sorrentino, G., Mazzarella, L. & Zagari, A. (2002). *Acta Cryst.* D**58**, 1695–1699.*

Betzel, C., Gourinath, S., Kumar, P., Kaur, P., Perbandt, M., Eschenburg, S. & Singh, T. P. (2001). *Biochemistry*, **40**, 3080–3088.*

Boggon, T. J., Chayen, N. E., Snell, E. H., Dong, J., Lautenschlager, P., Potthast, L., Siddons, D. P., Stojanoff, V., Gordon, E., Thompson, A. W., Zagalsky, P. F., Bi, R.-C. & Helliwell, J. R. (1998). *Philos. Trans. R. Soc. London Ser. A*, **356**, 1045–1061.*

Borgstahl, G. E. O., Vahedi-Faridi, A., Lovelace, J., Bellamy, H. D. & Snell, E. H. (2001). *Acta Cryst.* D**57**, 1204–1207.

Bosch, R., Lautenschlager, P., Potthast, L. & Stapelmann, J. (1992*a*). In *Proceedings of the VIIth European Symposium on Material and Fluid Sciences in Microgravity*, ESA SP-295. Paris: ESA.*

Bosch, R., Lautenschlager, P., Potthast, L. & Stapelmann, J. (1992*b*). *J. Cryst. Growth*, **122**, 310–316.*

Broutin, I., Riès-Kautt, M. & Ducruix, A. (1997). *J. Cryst. Growth*, **181**, 97–108.*

Broutin-L'Hermite, I., Riès-Kautt, M. & Ducruix, A. (2000). *Acta Cryst.* D**56**, 376–378.*

Cang, H. X. & Bi, R. C. (1999). *J. Cryst. Growth*, **196**, 442–446.*

Cang, H. X. & Bi, R.-C. (2001). *J. Cryst. Growth*, **232**, 473–480.

Carotenuto, L., Berisio, R., Castagnolo, D., Piccolo, C., Sorrentino, G., Tondonato, V., Vitagliano, L. & Zagari, A. (1999). *50th International Astronautical Federation Congress. Microgravity Sciences and Processes Symposium.* IAF-99-J.3.04.*

Carotenuto, L., Berisio, R., Piccolo, C., Vitagliano, L. & Zagari, A. (2001*a*). *Microgr. Space Stat. Util.* **2**, 72–74.*

Carotenuto, L., Berisio, R., Piccolo, C., Vitagliano, L. & Zagari, A. (2001*b*). *J. Cryst. Growth*, **232**, 481–488.*

Carotenuto, L., Castagnolo, D., Piccolo, C., Berisio, R., Vitagliano, L., Mazzarella, L. & Zagari, A. (2000). In *Proceedings of the First International Symposium on Microgravity Research and Applications in Physical Sciences and Biotechnology*, ESA SP-454. Paris: ESA.*

Carotenuto, L., Sica, F., Sorrentino, G. & Zagari, A. (1997). *J. Appl. Cryst.* **30**, 393–395.*

Carter, D. C., Lim, K., Ho, J. X., Wright, B. S., Miller, T. Y., Chapman, J., Keeling, K., Ruble, J., Vekilov, P. G., Thomas, B. R., Rosenberger, F. & Chernov, A. A. (1999). *J. Cryst. Growth*, **196**, 623–637.

Carter, D. C., Wright, B. *et al.* (1999). *J. Cryst. Growth*, **196**, 610–622.

Castagnolo, D., Carotenuto, L., Paduano, L., Vergara, A. & Sartorio, R. (2001). *J. Cryst. Growth*, **232**, 138–148.

Castagnolo, D., Vergara, A., Paduano, L., Sartorio, R. & Annunziata, O. (2002). *Acta Cryst.* D**58**, 1633–1637.*

Chayen, N. (1997). *Structure*, **5**, 1269–1274.

Chayen, N. (1998). *Acta Cryst.* D**54**, 8–15.*

Chayen, N. (2002). *Trends Biotechnol.* **20**, 98.*

Chayen, N. E., Gordon, E. J. & Zagalsky, P. F. (1996). *Acta Cryst.* D**52**, 156–159.*

Chayen, N. E. & Helliwell, J. R. (1999). *Nature (London)*, **398**, 20.*

Chayen, N., Shaw Stewart, P. D., Maeder, D. L. & Blow, D. (1990). *J. Appl. Cryst.* **23**, 297–302.

Chayen, N. E., Snell, E. H., Helliwell, J. R. & Zagalsky, P. F. (1997). *J. Cryst. Growth*, **171**, 219–225.*

Chernov, A. A. (1997). *J. Cryst. Growth*, **174**, 354.

Chernov, A. A., García-Ruiz, J. M. & Thomas, B. R. (2001). *J. Cryst. Growth*, **232**, 184–187.

Chernov, A. A. & Nishinaga, T. (1987). In *Morphology of Crystals*, edited by I. Sunegawa. Tokyo: Terra.

Chernov, A. A., Rashkovich, L. N., Smol'skii, I. L., Kuznetsov, Y. G.,

[1] Related websites are as follows. Databases of crystallization in μ*g*: http://www.esa.int/cgi-bin/mgdb, http://pcg.tecmasters.com/frames.html. APCF and other facilities for protein crystal growth: http://www.estec.esa.nl/spaceflight/map/ao/apcf.htm; http://spaceresearch.nasa.gov/research_projects/ros/apcf.html; http://lec.ugr.es/esatt/apcf/APCF.htm; http://pcg.tecmasters.com/equipment_1.html. Acceleration data from space missions: http://pims.grc.nasa.gov/html/ISSAccelerationArchive.html; http://www.grc.nasa.gov/WWW/MMAP/pdfs/Accelerometers.pdf. Protein crystallization under microgravity: http://microgravity.msfc.nasa.gov/snell/; http://otis.msfc.nasa.gov/image_archive/browse_bio.html; http://lec.ugr.es/esatt/toc.html; http://spec.ch.man.ac.uk/~eddie/microgravity.html.

Mkrtchyan, A. A. & Malkin, A. J. (1988). *Growth of Crystals*, edited by E. I. Givargizov & S. A. Grinberg, Vol. 15, pp. 43–91. NY/London: Consultants Bureau.
Dao-Thi, M.-H., Wyns, L., Poortmans, F., Bahassi, E. M., Couturier, M. & Loris, R. (1998). *Acta Cryst.* D**54**, 975–981.*
Dauter, Z., Lamzin, V. & Wilson, K. S. (1995). *Curr. Opin. Struct. Biol.* **5**, 784–790.
Decanniere, K., Transue, T. R., Desmyter, A., Maes, D., Muyldermans, S. & Wyns, L. (2001). *J. Mol. Biol.* **313**, 473–478.*
DeLucas, L. J. (2001). *Drug Discov. Today*, **6**, 734–744.*
DeLucas, L. J., Moore, K. M., Long, M. M., Rouleau, R., Bray, T., Crysel, W. & Weize, L. (2002). *J. Cryst. Growth*, **237–239**, 1646–1650.
Dieckmann, M. & Dierks, K. (2000). *SPIE International Symposium on Optical Science and Technology*, 4098A-02.*
Dieckmann, M., Dierks, K., Chayen, N., Smolik, G. & Stapelmann, J. (1997). *ESA: Preparing for the Future*, Vol. 7, pp. 6–7. Paris: ESA.*
Dixit, N. M., Kulkarni, A. M. & Zukoski, C. F. (2001). *Colloid Surf. A*, **190**, 47–60.
Dong, J., Boggon, T. J., Chayen, N. E., Raftery, J., Bi, R. C. & Helliwell, J. R. (1999). *Acta Cryst.* D**55**, 745–752.*
Dong, J., Pan, J., Wang, Y. & Bi, R.-C. (1998). *Space Med. Med. Eng.* **11**, 26–29.*
Ducruix, A. & Giegé, R. (1999). *Crystallization of Nucleic Acids and Proteins: A Practical Approach*, 2nd ed., edited by A. Ducruix & R. Giegé, pp. 1–435. Oxford: IRL Press.
Eschenburg, S., Degenhardt, M., Moore, K., DeLucas, L. J., Peters, K., Fittkau, S., Weber, W. & Betzel, C. (2000). *J. Cryst. Growth*, **208**, 657–664.*
Esposito, L., Sica, F., Berisio, R., Carotenuto, L., Giordano, A., Raia, C. A., Rossi, M., Lamzin, V. S., Wilson, K. S. & Zagari, A. (1997). *Proceedings of the LMS One Year Review Conference, Montreal, Canada.**
Esposito, L., Sica, F., Sorrentino, G., Berisio, R., Carotenuto, L., Giordano, A., Raia, C. A., Rossi, M., Lamzin, V. S., Wilson, K. S. & Zagari, A. (1998). *Acta Cryst.* D**54**, 386–390.*
Evrard, C., Declercq, J. P., Debaerdemaeker, T. & Konig, H. (1999). *Z. Kristallogr.* **214**, 427–429.*
Fourme, R., Ducruix, A., Riès-Kautt, M. & Capelle, B. (1995). *J. Synchrotron Rad.* **2**, 136–142.
Galkin, O. & Vekilov, P. (1999). *J. Phys. Chem. B*, **103**, 10965–10971.
García-Ruiz, J. M., Drenth, J., Riès-Kautt, M. & Tardieu, A. (2001). *A World Without Gravity: Research in Space for Health and Industrial Processes*, edited by G. Seibert, pp. 159–171. Paris: ESA.*
García-Ruiz, J. M., Gavira, J. A., Otálora, F., Guasch, A. & Coll, M. (1993). *Mat. Res. Bull.* **28**, 541–546.
García-Ruiz, J. M., Novella, M. L. & Otálora, F. (1999). *J. Cryst. Growth*, **196**, 703–710.*
García-Ruiz, J. M. & Otálora, F. (1997). *J. Cryst. Growth*, **182**, 155–167.*
García-Ruiz, J. M., Otálora, F., Novella, M. L., Gavira, J. A., Sauter, C. & Vidal, O. (2001). *J. Cryst. Growth*, **232**, 149–155.*
George, A., Chiang, Y., Guo, B., Arabshahi, A., Cai, Z. & Wilson, W. W. (1997). *Methods Enzymol.* **276**, 100–110.
Giegé, R., Drenth, J., Ducruix, A., McPherson, A. & Saenger, W. (1995). *Prog. Cryst. Growth Charact.* **30**, 237–281.*
Giegé, R. & McPherson, A. (2001). *International Tables for Crystallography*, Vol. F, edited by M. G. Rossmann & E. Arnold, pp. 81–99. Dordrecht: Kluwer Academic Press.*
Grant, M. L. & Saville, D. A. (1991). *J. Cryst. Growth*, **108**, 8–18.
Helliwell, J. R. (1988). *J. Cryst. Growth*, **90**, 259–272.
Henisch, H. K. (1988). *Crystals in Gels and Liesegang Rings*, p. 197. Cambridge University Press.
Kam, Z., Shore, H. B. & Feher, G. (1978). *J. Mol. Biol.* **123**, 539.
Kleywegt, G. J. & Jones, T. A. (2002). *Structure*, **10**, 465–472.
Klukas, O., Schubert, W.-D., Jordan, P., Krauss, N., Fromme, P., Witt, H. T. & Saenger, W. (1999*a*). *J. Biol. Chem.* **274**, 7361–7367.*
Klukas, O., Schubert, W.-D., Jordan, P., Krauss, N., Fromme, P., Witt, H. T. & Saenger, W. (1999*b*). *J. Biol. Chem.* **274**, 7351–7360.*
Ko, T.-P., Day, J. & McPherson, A. (2000). *Acta Cryst.* D**56**, 411–420.*
Ko, T.-P., Kuznetsov, Y. G., Malkin, A. J., Day, J. & McPherson, A. (2001). *Acta Cryst.* D**57**, 829–839.*
Koszelak, S., Day, J., Leja, C., Cudney, R. & McPherson, A. (1995). *Biophys. J.* **69**, 13–19.*
Kundrot, C. E., Judge, R. L., Pusey, M. L. & Snell, E. H. (2001). *Cryst. Growth Des.* **1**, 87–99.*
Kuznetsov, Y. G., Larson, S. B., Day, J., Greenwood, A. & McPherson, A. (2001). *Virology*, **284**, 223–234.*
Laubender, G., Krauss, N., Saenger, W., Frank, J. & Fromme, P. (2002). *9th International Conference on the Crystallization of Biological Macromolecules*, Jena, Germany.*
Lee, C. P. & Chernov, A. A. (2002). *J. Cryst. Growth*, **240**, 531–544.
Lin, H., Rosenberger, F., Alexander, J. I. D. & Nadarajah, A. (1995). *J. Cryst. Growth*, **151**, 153–162.
Lin, S.-X., Zhou, M., Azzi, A., Xu, G.-J., Wakayama, N. I. & Ataka, M. (2000). *Biochem. Biophys. Chem. Commun.* **275**, 274–278.
Lin, H., Petsev, S.-T., Thomas, B. R. & Vekilov, P. (2001). *Cryst. Growth Des.* **1**, 73–79.
Littke, W. & John, C. (1984). *Science*, **225**, 203–205.
Lorber, B. (2001). *Acta Cryst.* D**57**, 479.
Lorber, B. (2002). *Biochem. Biophys. Acta*, **1599**, 1–8.*
Lorber, B. & Giegé, R. (2001). *J. Cryst. Growth*, **231**, 252–261.*
Lorber, B. & Giegé, R. (1996). *J. Cryst. Growth*, **168**, 204–215.*
Lorber, B., Ng, J. D., Lautenschlager, P. & Giegé, R. (2000). *J. Cryst. Growth*, **208**, 665–677.*
Lorber, B., Sauter, C. & Giegé, R. (1999*a*). *Mutation Microgravité*, **13**, 1–3.*
Lorber, B., Sauter, C. & Giegé, R. (1999*b*). *Low G J.* **3**, 4–7.*
Lorber, B., Sauter, C., Ng, J. D. & Giegé, R. (1998). *EMBL Outstation Annual Report 1998*, edited by M. Wilmanns & V. Lamzin, p. 321–322. Hamburg: EMBL Outstation.*
Lorber, B., Sauter, C., Robert, M.-C., Capelle, B. & Giegé, R. (1999). *Acta Cryst.* D**55**, 1491–1494.*
Lorenz, S., Perbandt, M., Lippmann, C., Moore, K., DeLucas, L. J., Betzel, C. & Erdmann, V. (2000). *Acta Cryst.* D**56**, 498–500.*
Loris, R., Dao-Thi, M. H., Bahassi, E. M., Van Malderen, L., Poortmans, F., Liddington, R., Couturier, M. & Wyns, L. (1999). *J. Mol. Biol.* **285**, 1667–1677.*
McPherson, A. (1993). *J. Phys. D: Appl. Phys.* **26**, B104–B112.
McPherson, A. (1996). *Crystallogr. Rev.* **6**, 157–308.*
McPherson, A. (1997). *Trends Biotechnol.* **15**, 197–200.*
McPherson, A. (1999). *Crystallization of Biological Macromolecules*, p. 402. New York: Cold Spring Harbor Laboratory Press.
McPherson, A., Malkin, A. J., Kuznetsov, Y. J., Koszelak, S., Wells, M., Jenkins, G., Howard, J. & Lawson, G. (1999). *J. Cryst. Growth*, **196**, 572–586.
McPherson, A., Malkin, A. J., Kuznetsov, Y. G. & Plomp, M. (2001). *Acta Cryst.* D**57**, 1053–1060.
Malkin, A. J., Kuznetsov, Y. G. & McPherson, A. (1996). *J. Struct. Biol.* **117**, 124–137.*
Mapelli, M. & Tucker, P. A. (1999). *J. Struct. Biol.* **128**, 219–222.*
Mikol, V., Hirsch, E. & Giegé, R. (1990). *J. Mol. Biol.* **213**, 187–195.
Miller, T. Y., He, X. M. & Carter, D. C. (1992). *J. Cryst. Growth*, **122**, 306–309.
Miyashita, S., Komatsu, H., Suzuki, Y. & Nakada, T. J. (1994). *J. Cryst. Growth*, **141**, 419.
Ng, J. D., Lorber, B., Giegé, R., Koszelak, S., Day, J., Greenwood, A. & McPherson, A. (1997). *Acta Cryst.* D**53**, 724–733.*
Ng, J. D., Sauter, C., Lorber, B., Kirkland, N., Arnez, J. & Giegé, R. (2002). *Acta Cryst.* D**58**, 645–652.*
Otálora, F., Capelle, B., Ducruix, A. & García-Ruiz, J. M. (1999). *Acta Cryst.* D**55**, 644–649.*
Otálora, F. & García-Ruiz, J. M. (1997). *J. Cryst. Growth*, **182**, 141–154.*

Otálora, F., Novella, M. L., Gavira, J. A., Thomas, B. R. & García-Ruiz, J. M. (2001). *Acta Cryst.* D**57**, 412–417.*

Otálora, F., Novella, M. L., Rondon, D. & García-Ruiz, J. M. (1999). *J. Cryst. Growth*, **196**, 649–664.*

Otálora, F. & Vidal, O. (1998). *Ferritin, Apoferritin and Lysozyme Crystal Quality (Space Grown Crystals, STS-95 Mission)*. EMBL.*

Petsev, D. N., Thomas, B. R., Yau, S.-T. & Vekilov, P. (2000). *Biophys. J.* **78**, 2060–2069.

Pjura, P. E., Lenhoff, A. M., Leonard, A. G. & Gittis, A. G. (2000). *J. Mol. Biol.* **300**, 235–239.

Pletser, V., Minster, O., Bosch, R., Potthast, L. & Stapelmann, J. (2001*a*). In *Proceedings of the First International Symposium on Microgravity Research and Applications in Physical Sciences and Biotechnology*, ESA SP-454. Paris: ESA.*

Pletser, V., Minster, O., Bosch, R., Potthast, L. & Stapelmann, J. (2001*b*). *J. Cryst. Growth*, **232**, 439–449.*

Pletser, V., Stapelmann, J., Potthast, L. & Bosch, R. (1999). *J. Cryst. Growth*, **196**, 638–648.*

Riès-Kautt, M. (2001). *J. Phys. IV France*, **11**, 109–117.*

Riès-Kautt, M., Broutin, I., Ducruix, A., William, S., Kahn, R., Chayen, N., Blow, D., Paal, K., Littke, W., Lorber, B., Théobald-Dietrich, A. & Giegé, R. (1997). *J. Cryst. Growth*, **181**, 79–96.*

Riès-Kautt, M. & Ducruix, A. (1997). *Methods Enzymol.* **276**, 23–59.

Robert, M.-C., Capelle, B., Lorber, B. & Giegé, R. (2001). *J. Cryst. Growth*, **232**, 489–497.

Robert, M.-C., Vidal, O., García-Ruiz, J. M. & Otálora, F. (1999). *Crystallization of Nucleic Acids and Proteins: a Practical Approach* edited by A. Ducruix & R. Giegé, pp. 149–176. Oxford: IRL Press.*

Rodriguez-Fernandez, L., Stumpf, M., Haase, I., Fischer, M., Bacher, A. & Weinkauf, S. (2002). *9th International Conference on the Crystallization of Biological Macromolecules*, Jena, Germany.*

Saridakis, E. & Chayen, N. E. (2000). *Protein Sci.* **9**, 755–757.

Saridakis, E., Dierks, M., Moreno, K., Dieckmann, A. & Chayen, N. (2002). *Acta Cryst.* D**58**, 1597–1600.

Sauter, C., Lorber, B. & Giegé, R. (2002). *Proteins*, **48**, 146–150.*

Sauter, C., Otálora, F., Gavira, J. A., Vidal, O., Giegé, R. & García-Ruiz, J. M. (2001). *Acta Cryst.* D**57**, 1119–1126.*

Savino, R. & Monti, R. (1996). *J. Cryst. Growth*, **165**, 308–318.

Sheldrick, G. M. (1990). *Acta Cryst.* A**46**, 467–473.

Snell, E. H. (1997). *Proceedings of the Montreal Spacebound 1997 Meeting*, pp. 306–315. Canadian Space Agency.*

Snell, E. H., Boggon, T. J., Helliwell, J. R., Moskowitz, M. E. & Nadarajah, A. (1997). *Acta Cryst.* D**53**, 747–755.*

Snell, E. H., Cassetta, A., Helliwell, J. R., Boggon, T. J., Chayen, N. E., Weckert, E., Hölzer, K., Schroer, K., Gordon, E. J. & Zagalsky, P. F. (1997). *Acta Cryst.* D**53**, 231–239.*

Snell, E. H., Chayen, N. & Helliwell, J. R. (1999). *The Biochemist*, pp. 19–24.*

Snell, E. H., Helliwell, J. R., Boggon, T. J., Lautenschlager, P. & Potthast, L. (1996). *Acta Cryst.* D**52**, 529–533.*

Snell, E. H., Helliwell, J. R., Cassetta, T. J., Boggon, T. J., Weckert, E., Holzer, K., Schroer, K., Stojanoff, V. & Siddons, D. P. (1996). *Acta Cryst.* A**52**, C-517.*

Snell, E. H., Judge, R. A., Crawford, L., Forsythe, E. L., Pusey, M. L., Sportiello, M., Todd, P., Bellamy, H., Lovelace, J., Cassanto, J. M. & Borgstahl, G. E. O. (2001). *Cryst. Growth Des.* **1**, 151–158.*

Snell, E. H., Weisgerber, S., Helliwell, J. R., Weckert, E., Holzer, K. & Schroer, K. (1995). *Acta Cryst.* D**51**, 1099–1102.*

Snyder, R., Fuhrmann, K. & Walter, H. U. (1991). *J. Cryst. Growth*, **110**, 333–338.*

Stapelmann, J., Smolik, G., Lautenschlager, P., Lork, W. & Pletser, V. (2001). *J. Cryst. Growth*, **232**, 468–472.

Stojanoff, V., Siddons, D. P., Snell, E. H. & Helliwell, J. R. (1996). *Synchrotron Radiat. News*, **9**, 25–26.*

Tardieu, A., Le Verge, A., Malfois, M., Bonneté, F., Finet, S., Riès-Kautt, M. & Belloni, L. (1999). *J. Cryst. Growth*, **196**, 193–203.

Théobald-Dietrich, A., Lorber, B., Ng, J. D., Sauter, C., Charron, C., Robert, M.-C., Capelle, B. & Giegé, R. (2001). *Proceedings of the First International Symposium on Microgravity Research and Applications in Physical Sciences and Biotechnology*, ESA SP-454, pp. 457–463. Paris: ESA.*

Thiessen, J. K. (1994). *Acta Cryst.* D**50**, 491–495.

Thomas, B. R., Chernov, A. A., Vekilov, P. & Carter, C. W. Jr (2000). *J. Cryst. Growth*, **211**, 149–156.

Valiati, A. & Giglio, M. (1997). *Nature (London)*, **390**, 262–265.

Valiati, A. & Giglio, M. (1998). *Phys. Rev. E*, **58**, 4361–4371.

Vallazza, M., Banumathi, S., Perbandt, M., Betzel, C. & Erdmann, V. (2002). *9th International Conference on Crystallization of Biological Molecules*, Jena, Germany.*

Vallazza, M., Senge, A., Lippmann, C., Perbandt, M., Betzel, C., Bald, R. & Erdmann, V. (2001). *J. Cryst. Growth*, **232**, 340–352.*

Vaney, M. C., Broutin, I., Retailleau, P., Douangamath, A., Lafont, S., Hamiaux, C., Prange, T., Ducruix, A. & Riès-Kautt, M. (2001). *Acta Cryst.* D**57**, 929–940.*

Vaney, M. C., Maignan, S., Riès-Kautt, M. & Ducruix, A. (1996). *Acta Cryst.* D**52**, 505–517.*

Vekilov, P. & Alexander, J. I. D. (2000). *Chem. Rev.* **100**, 2061–2090.

Vekilov, P., Alexander, J. I. D. & Rosenberger, F. (1996). *Phys. Rev. E*, **54**, 6650–6660.

Vekilov, P. & Rosenberger, F. (1998). *Phys. Rev. Lett.* **80**, 2654–2656.

Vergara, A., Berisio, R., Vitagliano, L., Carotenuto, L., Piccolo, C., Sartorio, R. & Zagari, A. (2001). *Microgr. Space Stat. Util.* **2**, 73–75.*

Vergara, A., Corvino, E., Sorrentino, G., Carotenuto, L., Piccolo, C., Tortora, A., Mazzarella, L. & Zagari, A. (2002). *Acta Cryst.* D**58**, 1690–1694.*

Vergara, A., Paduano, L. & Sartorio, R. (2002). *Macromolecules*, **35**, 1389–1398.

Vergara, A., Paduano, L., Vitagliano, L. & Sartorio, R. (1999). *Phys. Chem. Chem. Phys.* **1**, 5377–5383.

Vergara, A., Paduano, L., Vitagliano, L. & Sartorio, R. (2000). *J. Phys. Chem. B*, **104**, 8086–8074.

Vidal, O., Bernard, Y., Robert, M.-C. & Lefaucheux, F. (1996). *J. Cryst. Growth*, **168**, 40–43.

Vidal, O., Robert, M.-C. & Boué, F. (1998). *J. Cryst. Growth*, **192**, 257–270.

Vivarès, D. & Bonneté, F. (2002). *Acta Cryst.* D**58**, 472–479.

Wagner, G. (1993). *Low G J.* **4**, 20–21.*

Wagner, G. (1994). *ESA J.* **18**, 25–32.*

Wagner, G. (1996). *Proceedings of the ESA Symposium on Space Station Utilization*, ESA SP-385. Paris: ESA.*

Wagner, G., Rotharmel, T., Perbandt, M. & Betzel, C. (1995). *DESY Yearbook*, pp. 503–504. Hamburg, Germany: DESY.*

Wagner, G. & Rotharmel, T. (1996). *Proceedings of the 9th European Symposium on Gravity-Dependent Phenomena in Physical Sciences, Berlin, 1995.**

Yau, S.-T., Petsev, D. N., Thomas, B. R. & Vekilov, P. (2000). *J. Mol. Biol.* **393**, 667–678.

Yoon, T.-S., Tetreault, S., Bosshard, H. E., Sweet, R. M. & Sygusch, J. (2001). *J. Cryst. Growth*, **232**, 520–535.

Zegers, I., Lah, N., Minh-Hao, D.-T. & Wyns, L. (2002). *9th International Conference on Crystallization of Biological Macromolecules*, Jena, Germany.*

Zhu, D.-W., Lorber, B., Sauter, C., Ng, J. D., Bénas, P., Le Grimellec, C. & Giegé, R. (2001). *Acta Cryst.* D**57**, 552–558.*

Zorb, C., Weisert, A., Stapelmann, J., Smolik, G., Carter, D. C., Wright, B. S., BrunnerJoos, K. D. & Wagner, G. (2002). *Microgr. Sci. Technol.* **13**, 3.*